Environmental and Climate Technologies

sciendo

RIGA TECHNICAL UNIVERSITY

2018, vol. 22, pp. 83–106
doi: 10.2478/rtuect-2018-0006
https://content.sciendo.com

Clayton Copula as an Alternative Perspective of Multi-Reaction Model

Alok DHAUNDIYAL[1]*, Suraj B. SINGH[2], Muammel M. HANON[3,4], Norbert SCHREMPF[5]

[1,4,5] *Mechanical Engineering Doctoral School, Szent Istvan University, Godollo, 2100, Hungary*

[2] *Department of Mathematics, Statistics & Computer Science, Govind Ballabh Pant University of Agriculture and Technology, Pantnagar, U.K., India*

[3] *Middle Technical University, Baquba Technical Institute, Baghdad, Iraq*

***Abstract* – This study proposes to assess the effect of some relevant parameters of biomass pyrolysis on the numerical solutions of n^{th} order distributed activation energy model (DAEM) or multi reaction model (MRM). The two-step process mechanisms of pyrolysis is described by replacing the initial distribution function of $f(E)$ with the Clayton copula. The upper limit (E_∞) of 'dE' integral, activation energy (A), heating rate (m), and the shape and scale parameters of bivariate distribution function. Temperature ramp rate is assumed to vary linearly with time. Thermo-analytical data is obtained with the help of thermogravimetric (TG) analysis. Asymptotic technique is adopted to approximate double exponential and bivariate distribution function $f(E_1, E_2)$, where E_1 and E_2 are the activation energies for bivariate scheme.**

***Keywords* – Asymptotic solution; biomass pyrolysis; bivariate function; distributed activation energy model; non-isothermal kinetics**

Nomenclature		
E_w	Step size width	kJ/mol
E_s	Central value	kJ/mol
$Y(x)$	Lambert function	–
$\Phi_p(E)$	The first marginal distribution function (Gaussian distribution)	–
$H(x)$	Heaviside step function	–
$R(x)$	Ramp function	–
m	Heating rate	°C/min
T	Temperature	°C
R	Universal gas constant	kJ/mol·K
DExp	Double exponential term	–
$f(E)$	Distribution function	–
$C(f(E_1), f(E_2))$	Copula function	–
$\Psi_p(E)$	The second marginal distribution function (Weibull distribution)	–

* Corresponding author.
E-mail address: alok.dext@hotmail.com

1. INTRODUCTION

Detrimental effect of conventional fuel on the environment made it indispensable to promote the energy conversion process of new renewable energy sources, such as forestry waste. The use of forest waste helps to alleviate the overdependence of fossil fuels resulting in carbon dioxide emissions, culpable for global warming, through its CO_2 balancing ability. Currently, pine needles have been recognized as one of the highly potential new renewable energy sources due to their adverse effect. However, it has some positive facets on mankind, but it is overlooked due to its combustible nature [1]–[5]. Pine needles can be transformed into thermal energy by means of thermochemical processes, such as pyrolysis, gasification and combustion. In the context of environmental factors; it is highly inflammable and has the ability to absorb plenty of water which in turn hinders the growth of fodder for livestock [1]. Keeping this concern in view, it becomes inevitable to evaluate its thermochemical behavior through its kinetic mechanism and explore the possibility to use it in real life, where as an alternative fuel it can also save the environment to some extent.

Pyrolysis represents one of the most important stages in all thermochemical processes, therefore, understanding and modeling its mechanism is a primary step to predict the behavior of the biomass during the whole process. During pyrolysis of the fuel, it decomposes into volatiles which comprise a major share of the pyrolysis products, and into a solid residue, the char. The volatiles consist of light gases (CH_4, CO_2, CO, C_2H_4), and others. The condensable species, tar and dust exist with unknown composition as they vary from biomass to biomass. As pyrolysis is a complex process due to large numbers of products, it becomes cumbersome to estimate the kinetic parameters through any kinetic model. Generally, it is defined as a two-step process [6], [7] in which the primary step takes place at a low temperature regime, which results in light, gas and tar. The secondary reactions occur at relatively elevated temperatures, where evolving of light gas and the aromatization of the biomass macromolecules result in char formation.

There are various models that are proposed to describe kinetics of thermal decomposition of biomass pyrolysis, which can be categorized as single and multi-reaction models. The iso-conversional method is one of the multi reaction models, which is independent of any reaction scheme, presumes that the Arrhenius parameters are not constant during the decomposition process but are the function of conversion and temperature. Moreover, an iso-conversional scheme relies on different heating rates and a solution is obtained as an average value of parameters. Another statistical approach is a model based method which relies on a predefined reaction mechanism or a phenomenological model and estimates kinetic parameters with high uncertainty in the final results [8]. However, the iso-conversional method is the most common mathematical scheme used for computation of kinetic parameters and developing a robust kinetic model, but it consumes appreciable time and resources. Moreover, in actual practice, the ratio E/R is significantly depended on extend of conversion X, and the plot to determine kinetic parameters is rarely linear. To tackle the aforementioned situation, the grey box modelling can be one of the alternative ways to describe kinetic reactions as continuous distribution functions of activation energies.

Comprehensive studies on these models are proposed in the literature [9]–[14]. The most reliable and accurate approach to model biomass pyrolysis is to implement the distributed activation energy model (DAEM) or multi-reaction model (MRM) [15]–[18]. The DAEM or MRM assume that a series of parallel reactions occur, having the common frequency factor and distinguished by a continuous distribution of the activation energies. In previous work, different forms of activation energy distribution functions are used to assess the influence of

kinetic parameters on the numerical solution [19]. Despite that, there are some major issues connected with solutions of the DAEM. In addition, the intrinsic description of pyrolysis as a single step process and as dichotomy of different pyrolysis steps is excluded from its non-generalized form. In this study, approximation of double exponential terms and simplification of double integral terms are carried out with the help of asymptotic techniques. Influence of some relevant parameters is investigated with the help of an extended model by using the bivariate distribution function instead of univariate, resulting in a model able to involve the likelihood of some other reactions which are of different activation energies. This bivariate approach is used to model biomass pyrolysis and gasification so that different classes of reactions can be brought under a single common equation. Behavior of this modified approach is applied to predict the behavior of loose biomass and the results are compared with methods that involve univariate functions. Interpretation of experimental data obtained by thermogravimetric analysis (TGA) is also performed to demonstrate the application of loose biomass through different perspectives. The classical DAEM is not able to describe different pyrolysis steps. To circumvent the demerit of previously performed analysis, this study has been proposed to see the variation obtained through combination of two different distribution functions with the help of the copula parameter (θ).

In addition, the results are compared with those obtained using single marginal distribution functions. Both models are used in the interpretation of experimental data derived from thermogravimetric analysis (TGA).

2. MATHEMATICAL SOLUTION OF MULTI-REACTION MODEL (MRM)

The DAEM belongs to the multi-reaction model, which postulates that many decomposition reactions take place. It can also be understood as a summation of an unlimited number of parallel single decomposition reactions, where each reaction is represented in the form:

$$\frac{dm_{\mathrm{i}}}{dt} = A_{\mathrm{i}} \exp\left(\frac{-E_{\mathrm{i}}}{RT}\right)(m_{\mathrm{i}}{}^{*} - m_{\mathrm{i}}), \tag{1}$$

where

i	one of several constituents;
$m_{\mathrm{i}}{}^{*}$	total released mass of i$^{\mathrm{th}}$ constituent;
t	time;
A_{i}	frequency factor.

If the number of reactions is large, it can be assumed that activation energies of these reactions are distributed, and therefore, it can be expressed as a function of the activation energy [4]. The derivation of the n^{th}-order DAEM can be found in the literature [20]. The non-isothermal n^{th}-order DAEM equation is expressed below.

First order reaction:

$$1 - X = \left\{\int_0^{\infty} \exp\left[\int_{T_0}^{T} \frac{-A}{m} \exp\left(\frac{-E}{RT}\right) dT\right] f(E), \tag{2}$$

n^{th} order reaction ($n \neq 1$):

$$1 - X = \left\{\int_0^{\infty} \left[1 - (1-n)\left(\frac{A}{m} \exp\left(\frac{-E}{RT}\right)\right) dT\right]^{\frac{1}{(1-n)}} f(E), \tag{3}$$

where

E	activation energy;
A	frequency factor;
n	reaction order;
T_0	initial reaction temperature;
X	mass fraction released during decomposition.

In this study, it is proposed to distinguish the single marginal distribution function from the bi-variate distribution function.

In previous studies, univariate functions, which can be either symmetric or asymmetric, are chosen as a distribution function for the molecular activation energies [4], [21]–[23]. Combining these univariate functions through Clayton copula is advantageous to determine the multi-dimensional dependence or existence of more than a class of reaction scheme. To compute DAEM, Eq. (2) and Eq. (3) are simplified individually.

The integrand in Eq. (2) comprised two different terms. The first part is a double exponential term (DExp) which varies with time through the temperature history experienced by the sample. On the other hand, the second term is invariant of time, but it depends on the distribution pattern of volatiles in the sample. The behavior of the temperature-dependent part, DExp, is simplified first, and thereafter, approximations are derived that are useful for solving physically feasible problems. The linear ramping temperature history along with the multi variant distributions of volatiles is perused. Simplification for these two terms, derived for Eq. (2), is also valid for the n^{th} order DAEM.

Approximations using double exponentials are performed below. Here, E can assume any positive value. The scheme adopted here is similar to that in Niksa and Lau [24], but involves more accurate and systematic approximations.

Invoking Eq. (2), we get:

$$\text{DExp} = \int_0^{\infty} \exp\left(\int_0^t -A\exp\left(\frac{-E}{Rml}\right) dl\right), \tag{4}$$

where temperature T (l) is related to time through Eq. (5) and l is the specific time at which temperature T is defined as:

$$T = T_0 + m \cdot l. \tag{5}$$

In order to propose the systematic simplifications of this integrand, it would be advantageous to assume the values of some parameters and functions on which it depends.

The frequency factors are typically in the range of $A \sim 10^{10}$–10^{13} s^{-1}, whereas the activation energies of interest lie in the domain of 100–300 kJ/mol. Variation of temperature depends on the particular experiments, but 800–1400 °C are typically used for gasification [1]. Although simplification performed for DAEM is also implemented for combustion problems where the temperature is appreciably high, it becomes easy to extrapolate the simplification made in higher temperature regimes.

Taking typical values, $E/RT_0 \sim 10$ while $tA \sim 10^{10}$. The large magnitude of both parameters makes the function rapidly varying with E.

The term inside the exponent of Eq. (4) can be solved by using the conventional Laplace approach where the parameter assumes to be $E/Rmt \to \infty$, therefore the integral term shows its influence at the neighborhood of $l \to t$ (and temperature is near its maximum). In this way, we will get the asymptotic approximation to the function:

$$\sim\exp\left(\frac{-ARmt^2}{E}e^{-\frac{E}{Rmt}}\right) \text{ as } \frac{E}{Rmt}\to\infty. \tag{6}$$

Eq. (6) can also be reformed as:

$$\exp\left(\frac{-ARmt^2}{E}e^{-\frac{E}{Rmt}}\right)\sim\exp\left(-\exp\left(\frac{E_s-E}{E_w}\right)\right). \tag{7}$$

Here, the exponential term varies rapidly from zero to one as the activation energy E increases by the step size E_w around E_s and this can be further approximated as discussed below.

Let $g(E)=\frac{E_s-E}{E_w}$, Eq. (7) becomes:

$$\sim\exp\left(-\exp\big(g(E)\big)\right),$$

where

$$g(E)\equiv\frac{-E}{Rmt}+\ln\left(\frac{ARmt^2}{E}\right).$$

As behavior of *g(E)* at the vicinity of E_s is of concern; hence, this function is expanded with the help of Taylor series about $E = E_s$:

$$g(E)\sim g(E_s)+(E-E_s)g'(E_s)+\cdots. \tag{8}$$

Using Eq. (8) and definition of $g(E)$, E_s and E_w are chosen so that:

$$g(E_s)=0 \text{ and } g'(E_s)=\frac{-1}{E_w}.$$

Solving these equations gives:

$$E_s=RmtY(At) \text{ and } E_w=\frac{RmtE_s}{Rmt+E_s},$$

where Y(x) is the Lambert W function.

In order to simplify it further, introduce the energy rescaling factor 'y':

$$y=\frac{E}{E_0},\ y_s=\frac{E_s}{E_0},\ y_w=\frac{E_w}{E_0},$$

where

E_0 the mean activation energy;

τ the time rescaling factor $\tau=At$, then:

$$y_s=\frac{RmtY(\tau)}{AE_0} \text{ and } y_w=\frac{y_s}{1+Y(\tau)}.$$

2.1. Distribution Pattern

In Eq. (1) and Eq. (2), DExp is multiplied by the initial distribution, which is substituted by the Clayton copula. In order to simplify the bi-variant function, the mean (E_0) and the variance (σ^2) of marginal distribution functions are assumed to be equal (both of which are constant). In this study, the combination of symmetric and asymmetric distribution functions is adopted to evaluate the dependence of the remaining mass proportion on activation energies, associated with primary and secondary reactions. On the other hand, limits imposed on the distribution pattern are demarcated with respect to the width of DExp. One is relatively wide initial distribution compared with the width of DExp, whereas the other has a relatively narrow width than that of DExp. Behavior of the total integrand changes with time is mainly dependent on the applied limit. When the initial distribution is relatively wide as compared to E_w, the total integrand acts in a way that is similar to the initial distribution function. As the time proceeds, it is progressively chopped off from the left hand side by the step-like function, DExp. The position of the maximum of total integrand shifts significantly, and the shape of the curve tends to be asymmetric. On the other hand, if the width of initial distribution is relatively narrower than the width of DExp, the total integrand is surpassed by the initial distribution with amplitude that is progressively reduced by DExp as time proceeds. The shape of the curve remains more symmetrical than that of wide distribution limit, but the location of its maximum is not stationary with respect to time, and therefore, there is always a need to find the maximum of the total integrand in each iterative loop. Here, the study is pivoted around the wide distribution limit only. The mode of thermal analysis also affects the shape of the curve. For example, in case of the isothermal condition (constant temperature), the amount of release of volatiles with respect to time begins to change perceptibly even at a very early stage. However, in case of ramping temperature, the location of the central value, E_s, moves with time in a similar way to the constant temperature, with the logarithmic term is replaced by a Lambert W function [5], [25]. Moreover, the effect of temperature on the width of DExp, E_w (= $E_0 \cdot y_w$), is narrow at the beginning. This factor led to major differences in the appearances of the curves denoting the release volatile with time between the ramping and constant temperature profile. In the ramping temperature case, the amount of released volatile does not perceive until the critical time is reached when the two parts of the total integrand overlap significantly. Eq. (9) represents the critical time required to see the variation:

$$t_c = \frac{t_{max}+t_{min}}{2}. \tag{9}$$

Here, t_{min} is the time when DExp just begins to encounter the distribution, whereas t_{max} denotes the time when DExp has just moved past the distribution

Note: The ramping temperature case can easily be generalized to the case of a nonzero initial temperature T_0, by simply replacing t with $t + T_0/m$ everywhere.

2.2. Wide Distribution Case

In this case, the initial distribution is relatively wider than DExp. DExp varied from zero to one in the neighborhood of $y = y_s$ and has previously been approximated by the step-function [26]–[29]:

$$H(y - y_s) = \begin{cases} 0, y < y_s \\ 1, y \geq y_s \end{cases}.$$

3. APPLICATION OF CLAYTON COPULA AS A DISTRIBUTION FUNCTION

Adopting a copula approach is not only limited to the risk management problem, but it also provides better insight into the engineering system, hence, repairing engineering units that can either be preventive or corrective. Copula eases complex situations where more than two sub-unit working conditions are to be analyzed within the main structure. Some examples of repairing related problems have been reviewed in the literature [30]–[32]. Moreover, the benefit of using Clayton copula is known by the fact that it has remarkable invariance under truncation [33].

To correlate different regime of biomass pyrolysis, there is a requirement of an initial distribution function which can easily and accurately be modeled through a multi-reaction model as it is indispensable to involve all sets of reactions that affect the remaining mass proportion of volatiles. Pyrolysis of biomass is significantly dependent on the reaction scheme and local temperature. However, the overall reaction mechanism of pyrolysis is very complicated due to the high number of products that are not easily recognized during experimentation, but postulation and simplification of the existing models provide alternative means to form different models. To describe the behavior of loose biomass, some variation is done to include the effect of relevant parameters on pyrolysis of biomass. Interdependence of various reactions on each other cannot be properly predicted by a single distribution function, therefore, a bivariate function is used as a substitute of the initial distribution function of molecular activation energies, so that it can be comprehended as an alternative method to solve the DAEM. The impact of this study can also be understood by the fact that the classical formulation is not able to distinguish between the different pyrolysis steps. Dhaundiyal and Tewari [5] have proposed an alternative method to analyze DAEM through trifurcation of biomass into its major constitutes, but the computational problem became cumbersome when a different algorithm for each of the constituents has to be made. Such intrinsic interpretation of pyrolysis as a single step process can be eliminated, to some extent, through marginal distribution functions which can be either symmetric, asymmetric, or a combination of the two. Several other methods are also proposed to counter the implications that arise during pyrolysis of biomass. One of them is a second Gaussian distribution (2-DAEM) [34]. This multi-Gaussian approach was also used by Zhang et al. [35] to model biomass pyrolysis and gasification by using a different distribution of activation energy for each decomposition reactions that share the same frequency factor. Yang and his co-worker [36] implemented the same scheme to predict the behavior of selective fuel.

Without making the integral process more complicated, there is also the likelihood of existence of multivariate distribution function within DAEM. Molecular activation energies of different reaction steps can be bifurcated and represented by coupling of a different nature of marginal probability distribution. Moreover, it also overcomes the demerit of 2-DAEM that only uses the symmetrical distribution functions to interpret the experimental data, but it is not necessary for thermoanalytical data to exhibit the same nature. Experimental results are significantly dicey and cannot be interpreted with a particular class of distribution function, as it is not necessary that thermo-analytical data is symmetric about the mean, therefore, there is always some skewness present in the experimental data. Application of copula provides a wide variety of combination of asymmetric and symmetric functions. However, it is difficult to seek the exactness through any approximation technique, but the differences between different perspectives to model biomass pyrolysis may be abridged through the proper selection of distribution functions.

For fruition of the proposed scheme, Sklar delivered an effective way to model the dependent structure of random parameters with the assistance of copula functions. To solve this problem, the Archimedean families of copulas have been chosen as an alternative distribution pattern of activation energies. The well-known representatives of the Archimedian family are Gumbel–Hougaard and Frank and Clayton copulas.

A copula function may be represented as a cumulative probability function of activation energies (E_1, E_2). Now suppose $E \in (E_1, E_2)$ and $f(E_1)$ and $f(E_2)$ are any two univariate distributions, expressed as:

$$f(E_1, E_2) = C\big(f(E_1);\, f(E_2)\big), \tag{10}$$

where C is the copula used to join the univariate margins $f(E_1)$ and $f(E_2)$.

Let $f(E_1) = \Phi_p(E)$ and $f(E_2) = \Psi_p(E)$.

Here, $\Phi_p(E)$ represents the Gaussian distribution function and $\Psi_p(E)$, assumed to denote the two-parameter Weibull distribution as expressed below:

$$\Phi_p(E) = \frac{1}{\sqrt{2\pi\sigma^2}} \mathrm{e}^{-\left(\frac{(E-E_0)^2}{2\sigma^2}\right)}, \tag{11}$$

$$\Psi_p(E) = \frac{\beta}{\eta}\left(\frac{E}{\eta}\right)^{(\beta-1)} \mathrm{e}^{-\left(\frac{E}{\eta}\right)^{\beta}}, \tag{12}$$

where

E_0 denotes the mean activation energy, kJ/mol;

σ^2 the variance of the Gaussian distribution and function, kJ/mol;

β and η the shape and scale parameters of the Weibull distribution, respectively, kJ/mol.

3.1. Case A: First Order Reaction (n = 1) and θ = 1 (Refer Appendix A)

$$(1-X) \sim \int_0^{\infty} \exp\left[\int_{T_0}^{T} \frac{-A}{m} \exp\left(\frac{-E}{RT}\right) \mathrm{d}T\right] \Big(1 - \big(\Phi_p(E) + \Psi_p(E) + 2\big) + \big(\Phi_p(E) + \Psi_p(E) + 2\big)^2 + \cdots\Big)\, dE, \tag{13}$$

$$\begin{aligned} &\sim 3\int_0^{\infty} \exp\left[\int_{T_0}^{T} \frac{-A}{m} \exp\left(\frac{-E}{RT}\right) dT\right] dE + \int_0^{\infty} \exp\left[\int_{T_0}^{T} \frac{-A}{m} \exp\left(\frac{-E}{RT}\right) dt\right] \left(\frac{1}{\sqrt{2\pi\sigma^2}} e^{-\left(\frac{(E-E_0)^2}{2\sigma^2}\right)}\right)^2 dE \\ &\quad + \int_0^{\infty} \exp\left[\int_{T_0}^{T} \frac{-A}{m} \exp\left(\frac{-E}{RT}\right) dT\right] \left(\frac{\beta}{\eta}\left(\frac{E}{\eta}\right)^{(\beta-1)} e^{-\left(\frac{E}{\eta}\right)^{\beta}}\right)^2 dE \\ &\quad + 2\int_0^{\infty} \exp\left[\int_{T_0}^{T} \frac{-A}{m} \exp\left(\frac{-E}{RT}\right) dT\right] \frac{1}{\sqrt{2\pi\sigma^2}} e^{-\left(\frac{(E-E_0)^2}{2\sigma^2}\right)} \frac{\beta}{\eta}\left(\frac{E}{\eta}\right)^{(\beta-1)} e^{-\left(\frac{E}{\eta}\right)^{\beta}} dE \\ &\quad + 3\int_0^{\infty} \exp\left[\int_{T_0}^{T} \frac{-A}{m} \exp\left(\frac{-E}{RT}\right) dT\right] \left(\frac{1}{\sqrt{2\pi\sigma^2}} e^{-\left(\frac{(E-E_0)^2}{2\sigma^2}\right)} + \frac{\beta}{\eta}\left(\frac{E}{\eta}\right)^{(\beta-1)} e^{-\left(\frac{E}{\eta}\right)^{\beta}}\right) dE + \ldots \end{aligned} \tag{14}$$

Applying Heaviside step function in Eq. (14), we have:

$$\begin{aligned}(1-X)\sim 3R(y_s)+\frac{1}{2}\left(3+\sqrt{\frac{\alpha}{2\pi}}\right)erfc\left(\sqrt{\alpha}(y_s-1)\right)+(1-K)\\ +2(1-M)+3(1-S)+3\int_0^{\infty}E_0\left[\exp\left(-\exp\left(\frac{y_s-y}{y_w}\right)\right)-H(y-y_s)\right]dy\\ +\int_0^{\infty}\frac{\alpha}{\pi}\left[\exp\left(-\exp\left(\frac{y_s-y}{y_w}\right)\right)-H(y-y_s)\right]e^{-2\left(\alpha(y-1)^2\right)}dy\\ +\int_0^{\infty}\left[\exp\left(-\exp\left(\frac{y_s-y}{y_w}\right)\right)-H(y-y_s)\right]\beta^2 s^{2\beta}y^{2(\beta-1)}e^{-2(sy)^{\beta}}dy\\ +2\int_0^{\infty}\left[\exp\left(-\exp\left(\frac{y_s-y}{y_w}\right)\right)-H(y-y_s)\right]\left(\sqrt{\frac{\alpha}{\pi}}\right)\beta s^{\beta}(y)^{\beta-1}e^{-\left(\alpha(y-1)^2+(sy)^{\beta}\right)}dy\\ +3\int_0^{\infty}\left[\exp\left(-\exp\left(\frac{y_s-y}{y_w}\right)\right)-H(y-y_s)\right]\left(\sqrt{\frac{\alpha}{\pi}e^{-\left(\alpha(y-1)^2\right)}+\beta s^{\beta}(y)^{(\beta-1)}e^{-(sy)^{\beta}}}\right)dy+\cdots.\end{aligned} \tag{15}$$

It is to be noted that the distribution functions are multiplied by the functions that are negligibly small everywhere except in the neighborhood of size y_w around the point $y = y_s$, therefore, these functions can be approximated by expanding the initial distribution term with the help of Taylor series.

Let $\left(\frac{y-y_s}{y_w}\right) = x$ and $f(y) = y^{(\beta-1)}\exp\{-(sy)^{\beta}\}$.

Expanding $f(y)$ and $e^{-(\alpha(y-1)^2)}$ with the help of Taylor series about $y = y_s$, we have:

$$\begin{aligned}f(y) = (y_s)^{(\beta-1)}\exp\left(-(\alpha y_s)^{\beta}\right)\left[1-\frac{x(y_w)}{y_s}\left(\beta-\beta(sy_s)^{\beta}-1\right)+\left(\frac{x(y_w)}{y_s}\right)^2\left(\beta^2\left(-3(sy_s)^{\beta}\right.\right.\right.\\ +(sy_s)^{2\beta}+1\big)+3\lambda\big((sy_s)^{\beta}-1\big)+2\big)-\left(\frac{x(y_w)}{y_s}\right)^3\left(s^2\beta^4(-y_s{}^2)\big((sy_s)^{\beta}-1\big)\right.\\ +\beta^3\big(-(sy_s)^2-7(sy_s)^{\beta}+3(sk_s)^{2\beta}+1\big)-3\lambda^2\big(-6(sy_s)^{\lambda}+(sy_s)^{2\lambda}+2\big)\\ \left.\left.-11\lambda\big((sy_s)^{\lambda}-1\big)-6\big)\right].\end{aligned}$$

Substituting the value of $f(y)$ in Eq. (15), we get:

$$\sim 3\left(A_0E_0 + R(y_s)\right) + \frac{1}{2}\left(3 + \sqrt{\frac{\alpha}{2\pi}}\right) erfc\left(\sqrt{\alpha}(y_s - 1)\right) + (1 - K) + 2(1 - M) + 3(1 - S)$$
$$+3\left[\sqrt{\frac{\alpha}{\pi}} y_w e^{-\alpha(y_s-1)^2}\left(A_0 - 2\alpha y_w(y_s - 1)A_1 + \alpha {y_w}^2\{2\alpha(y_s - 1)^2 - 1\}A_2 + \frac{2}{3}{y_w}^3\alpha^2\{2(y_s\right.\right.$$
$$-1) + 2\alpha(y_s - 1)^3 + 1\}A_3\Big) + \beta s^\beta (y_s)^{(\beta-1)}\exp\left(-(\alpha y_s)^\beta\right)\left(A_0 - \frac{(y_w)}{y_s}\left(\beta - \beta(sy_s)^\beta\right.\right.$$
$$-1)A_1 + \left(\frac{(y_w)}{y_s}\right)^2 \left(\beta^2\left(-3(sy_s)^\beta + (sy_s)^{2\beta} + 1\right) + 3\lambda\left((sy_s)^\beta - 1\right) + 2\right)A_2$$
$$-\left(\frac{(y_w)}{y_s}\right)^3 A_3\left(s^2\beta^4(-{y_s}^2)\left((sy_s)^\beta - 1\right) + \beta^3\left(-(sy_s)^2 - 7(sy_s)^\beta + 3(sk_s)^{2\beta} + 1\right)\right.$$
$$\left.\left.-3\lambda^2\left(-6(sy_s)^\lambda + (sy_s)^{2\lambda} + 2\right) - 11\lambda\left((sy_s)^\lambda - 1\right) - 6\right)\right)\Big] + \left[\frac{\alpha}{\pi} y_w e^{-2\alpha(y_s-1)^2}\left(A_0\right.\right.$$
$$-4\alpha y_w(y_s - 1)A_1 + 2\alpha {y_w}^2\{4\alpha(y_s - 1)^2 - 1\}A_2 + \frac{8}{3}{y_w}^3\alpha^2\{2(y_s - 1) + 4\alpha(y_s - 1)^3$$
$$+1\}A_3\Big) + \left(\beta^2 s^{2\beta}(y_s)^{2(\beta-1)}\exp\left(-(sy_s)^{2\beta}\right)\left(A_0 - 2A_1\frac{y_w}{y_s}\left(\beta\left((sy_s)^\beta - 1\right) + 1\right)\right.\right. \quad (16)$$
$$+A_2\left(\frac{y_w}{y_s}\right)^2\left(\beta^2\left(2 + 2(sy_s)^{2\beta} - 5(sy_s)^\beta\right) + 5\beta\left((sy_s)^\beta - 1\right) + 3\right) + \frac{A_3}{3}\left(\frac{y_w}{y_s}\right)^3\left(\beta^3\left(4\right.\right.$$
$$-4(sy_s)^{3\beta} + 18(sy_s)^{2\beta} - 19(sy_s)^\beta\right) - 9\beta^2\left(2 + 2(sy_s)^{2\beta} - 5(sy_s)^\beta\right) - 26\beta\left((sy_s)^\beta - 1\right)$$
$$\left.\left.\left.-12\right)\right)\right)\Big] + 2\left[\beta s^\beta\sqrt{\frac{\alpha}{\pi}}\left((y_s)^{\beta-1}e^{-\left(\alpha(y_s-1)^2 + (sy_s)^\beta\right)}\left(A_0 + A_1\frac{y_w}{y_s}\left(-\beta(sy_s)^\beta + \beta\right.\right.\right.$$
$$-2\alpha(y_s - 1)y_s - 1\Big) + \frac{1}{2}A_2\left(\frac{y_w}{y_s}\right)^2\left(\beta^2\left(-3(sy_s)^\beta + (sy_s)^{2\beta} + 1\right) + \beta(4\alpha y_s(y_s - 1)\right.$$
$$+3)\left((sy_s)^\beta - 1\right) + 4\alpha^2{y_s}^2(y_s - 1)^2 + 2\alpha y_s(y_s - 1) + 2\Big) + \frac{1}{6}A_3\left(\frac{y_w}{y_s}\right)^3\Big)\Big(\beta^3\left(-\left(7(sy_s)^\beta\right.\right.$$
$$\left.-6(sy_s)^{2\beta} + (sy_s)^{3\beta} - 1\right)\Big) - 6\beta^2(\alpha(y_s - 1)y_s + 1)\left(1 + (sy_s)^{3\beta} - 3(sy_s)^\beta\right)$$
$$-\beta(11 + 6y_s\alpha(2y_s - 3) + 12(y_s\alpha)^2(y_s - 1)^2 + 6\alpha y_s(2y_s - 3) + 11)\left((sy_s)^\beta - 1\right)$$
$$\left.\left.-2\left(4\left(\alpha y_s(y_s - 1)\right)^3 - 6\left(\alpha y_s(y_s - 1)\right)^2 + 3\alpha y_s(y_s - 1) + 3\right)\right) + \cdots\Big)\Big].$$

3.2. Case B: First Order Reaction (n = 1) and θ = 2 (Refer Appendix A)

$$(1 - X)\sim \int_0^\infty \exp\left[\int_{T_0}^T \frac{-A}{m}\exp\left(\frac{-E}{RT}\right)dT\right]\left(1 - \left(\Phi_P(E) + \Psi_p(E) + 2\right) + \frac{3}{2}\left(\Phi_P(E) + \Psi_p(E)\right.\right. \quad (17)$$
$$\left.\left.+2\right)^2\right) + \cdots.$$

$$(1 - X)\sim 5\int_0^\infty \exp\left[\int_{T_0}^T \frac{-A}{m}\exp\left(\frac{-E}{RT}\right)dT\right]$$
$$+\frac{3}{2}\left(\int_0^\infty \exp\left[\int_{T_0}^T \frac{-A}{m}\exp\left(\frac{-E}{RT}\right)dT\right]\left(\frac{1}{\sqrt{2\pi\sigma^2}}e^{-\left(\frac{(E-E_0)^2}{2\sigma^2}\right)}\right)^2\right.$$
$$\left.+\int_0^\infty \exp\left[\int_{T_0}^T \frac{-A}{m}\exp\left(\frac{-E}{RT}\right)dT\right]\left(\frac{\beta}{\eta}\left(\frac{E}{\eta}\right)^{(\beta-1)}e^{-\left(\frac{E}{\eta}\right)^\beta}\right)^2\right) \quad (18)$$
$$+3\int_0^\infty exp\left[\int_{T_0}^T \frac{-A}{m}exp\left(\frac{-E}{RT}\right)dT\right]\frac{1}{\sqrt{2\pi\sigma^2}}e^{-\left(\frac{(E-E_0)^2}{2\sigma^2}\right)}\frac{\beta}{\eta}\left(\frac{E}{\eta}\right)^{(\beta-1)}e^{-\left(\frac{E}{\eta}\right)^\beta}$$
$$+5\int_0^\infty exp\left[\int_{T_0}^T \frac{-A}{m}exp\left(\frac{-E}{RT}\right)dT\right]\left(\frac{1}{\sqrt{2\pi\sigma^2}}e^{-\left(\frac{(E-E_0)^2}{2\sigma^2}\right)} + \frac{\beta}{\eta}\left(\frac{E}{\eta}\right)^{(\beta-1)}e^{-\left(\frac{E}{\eta}\right)^\beta}\right) + \cdots.$$

Using Heaviside step function in Eq. (19), we have:

$$(1-X)\sim 5\left(A_0E_0+R(y_s)\right)+\frac{1}{2}\left(5+3\sqrt{\frac{\alpha}{2\pi}}\right)erfc\left(\sqrt{\alpha}(y_s-1)\right)+\frac{3}{2}(1-K)+3(1-M)$$
$$+5(1-S)+5\int_0^{\infty}E_0\left[\exp\left(-\exp\left(\frac{y_s-y}{y_w}\right)\right)-H(y-y_s)\right]dy+\frac{3}{2}\left(\int_0^{\infty}\frac{\alpha}{\pi}\left[\exp\left(-\exp\left(\frac{y_s-y}{y_w}\right)\right)\right.\right.$$
$$\left.-H(y-y_s)\right]e^{-2\alpha(y-1)^2}dy+\int_0^{\infty}\left[\exp\left(-\exp\left(\frac{y_s-y}{y_w}\right)\right)-H(y\right.$$
$$\left.-y_s)\right]\beta s^{\beta}(y)^{2(\beta-1)}e^{-(sy)^{2\beta}}\,dy\Big)+3\int_0^{\infty}\left[\exp\left(-\exp\left(\frac{y_s-y}{y_w}\right)\right)-H(y\right.$$
$$\left.-y_s)\right]\left(\sqrt{\frac{\alpha}{\pi}}\frac{\beta}{\eta}(sy)^{\beta-1}e^{-(\alpha(y-1)^2+(sy)^{\beta})}dy+5\int_0^{\infty}\left[\exp\left(-\exp\left(\frac{y_s-y}{y_w}\right)\right)-H(y\right.\right.$$
$$\left.\left.-y_s)\right]\left(\sqrt{\frac{\alpha}{\pi}}e^{-\alpha(y-1)^2}+\beta s^{\beta}(y)^{(\beta-1)}e^{-(sy)^{\beta}}\right)\,dy\,, \tag{19}$$

$$\sim 5\left(A_0E_0+R(y_s)\right)+\frac{1}{2}\left(5+3\sqrt{\frac{\alpha}{2\pi}}\right)erfc\left(\sqrt{\alpha}(y_s-1)\right)+5(1-K)+\frac{3}{2}(1-M)+3(1-S)$$
$$+5\left[\sqrt{\frac{\alpha}{\pi}}y_we^{-\alpha(y_s-1)^2}\left(A_0-2\alpha y_w(y_s-1)A_1+\alpha {y_w}^2\{2\alpha(y_s-1)^2-1\}A_2\right.\right.$$
$$\left.+\frac{2}{3}{y_w}^3\alpha^2\{2(y_s-1)+2\alpha(y_s-1)^3+1\}A_3\right)+\beta s^{\beta}\,(y_s)^{(\beta-1)}\exp\left(-(\alpha y_s)^{\beta}\right)\left(A_0\right.$$
$$-\frac{(y_w)}{y_s}\left(\beta-\beta(sy_s)^{\beta}-1\right)A_1+\left(\frac{(y_w)}{y_s}\right)^2\left(\beta^2\left(-3(sy_s)^{\beta}+(sy_s)^{2\beta}+1\right)+3\lambda\left((sy_s)^{\beta}-1\right)\right.$$
$$\left.+2\right)A_2-\left(\frac{(y_w)}{y_s}\right)^3A_3\left(s^2\beta^4(-{y_s}^2)\left((sy_s)^{\beta}-1\right)+\beta^3\left(-(sy_s)^2-7(sy_s)^{\beta}+3(sk_s)^{2\beta}+1\right)\right.$$
$$\left.\left.-3\lambda^2\left(-6(sy_s)^{\lambda}+(sy_s)^{2\lambda}+2\right)-11\lambda\left((sy_s)^{\lambda}-1\right)-6\right)\right]+\frac{3}{2}\left[\frac{\alpha}{\pi}y_we^{-2\alpha(y_s-1)^2}\left(A_0\right.\right.$$
$$-4\alpha y_w(y_s-1)A_1+2\alpha {y_w}^2\{4\alpha(y_s-1)^2-1\}A_2+\frac{8}{3}{y_w}^3\alpha^2\{2(y_s-1)+4\alpha(y_s-1)^3$$
$$\left.+1\}A_3\right)+\left(\beta^2s^{2\beta}(y_s)^{2(\beta-1)}\exp\left(-(sy_s)^{2\beta}\right)\left(A_0-2A_1\frac{y_w}{y_s}\left(\beta\left((sy_s)^{\beta}-1\right)+1\right)\right.\right.$$
$$+A_2\left(\frac{y_w}{y_s}\right)^2\left(\beta^2\left(2+2(sy_s)^{2\beta}-5(sy_s)^{\beta}\right)+5\beta\left((sy_s)^{\beta}-1\right)+3\right)+\frac{A_3}{3}\left(\frac{y_w}{y_s}\right)^3\left(\beta^3(4\right.$$
$$-4(sy_s)^{3\beta}+18(sy_s)^{2\beta}-19(sy_s)^{\beta})-9\beta^2\left(2+2(sy_s)^{2\beta}-5(sy_s)^{\beta}\right)-26\beta\left((sy_s)^{\beta}-1\right)$$
$$\left.\left.\left.-12\right)\right)\right)\Big]+3\left[\beta s^{\beta}\sqrt{\frac{\alpha}{\pi}}\left((y_s)^{\beta-1}e^{-(\alpha(y_s-1)^2+(sy_s)^{\beta})}\left(A_0+A_1\frac{y_w}{y_s}\left(-\beta(sy_s)^{\beta}+\beta\right.\right.\right.\right.$$
$$\left.-2\alpha(y_s-1)y_s-1\right)+\frac{1}{2}A_2\left(\frac{y_w}{y_s}\right)^2\left(\beta^2\left(-3(sy_s)^{\beta}+(sy_s)^{2\beta}+1\right)+\beta(4\alpha y_s(y_s-1)\right.$$
$$\left.+3)\left((sy_s)^{\beta}-1\right)+4\alpha^2{y_s}^2(y_s-1)^2+2\alpha y_s(y_s-1)+2\right)+\frac{1}{6}A_3\left(\frac{y_w}{y_s}\right)^3\Big)\Big(\beta^3\left(-\left(7(sy_s)^{\beta}\right.\right.$$
$$\left.-6(sy_s)^{2\beta}+(sy_s)^{3\beta}-1\right)\Big)-6\beta^2(\alpha(y_s-1)y_s+1)\left(1+(sy_s)^{3\beta}-3(sy_s)^{\beta}\right)$$
$$-\beta(11+6y_s\alpha(2y_s-3)+12(y_s\alpha)^2(y_s-1)^2+6\alpha y_s(2y_s-3)+11)\left((sy_s)^{\beta}-1\right)$$
$$\left.\left.-2\left(4\left(\alpha y_s(y_s-1)\right)^3-6\left(\alpha y_s(y_s-1)\right)^2+3\alpha y_s(y_s-1)+3\right)\right)+\cdots\right)\Big]. \tag{20}$$

3.3. Case C: n^{th} Order reaction ($n \neq 1$) and $\theta = 1$

For getting a solution of n^{th} order reaction, invoke Eq. (3):

$$(1(X)_{n^{\text{th}}} = \int_0^{\infty} \left[1-(1-n)\int_{T_0}^{T}\left(\frac{A}{m}\exp\left(\frac{-E}{RT}\right)\right)dT\right]^{\frac{1}{(1-n)}} \left(1-\left(\Phi_{\text{P}}(E)+\Psi_{\text{p}}(E)+2\right) + \left(\Phi_{\text{P}}(E)+\Psi_{\text{p}}(E)+2\right)^2+\cdots\right)dE\,.$$

Expanding the first integral term by using the binomial theorem, we have:

$$(1\,X)_{n^{\text{th}}} \sim \int_0^{\infty}\left[\left(1-\int_{T_0}^{T}\left(\frac{A}{m}\exp\left(\frac{-E}{RT}\right)\right)dT+\frac{n}{2}\left(\int_{T_0}^{T}\left(\frac{A}{m}exp\left(\frac{-E}{RT}\right)\right)dT\right)^2+\cdots\right)dT\right]\left(3 +3\left(\Phi_{\text{P}}(E)+\Psi_{\text{p}}(E)\right)+\left(\Phi_{\text{P}}(E)+\Psi_{\text{p}}(E)\right)^2+\cdots\right)dE\,, \tag{21}$$

$$\begin{aligned}((1\,X)_{n^{\text{th}}} \sim \int_0^{\infty}&\left(3\left(1-\int_{T_0}^{T}\left(\frac{A}{m}exp\left(\frac{-E}{RT}\right)\right)dT+\frac{n}{2}\left(\int_{T_0}^{T}\left(\frac{A}{m}exp\left(\frac{-E}{RT}\right)\right)dT\right)^2+\cdots\right)\right)\text{dE}\\ +3\int_0^{\infty}&\left(1-\int_{T_0}^{T}\left(\frac{A}{m}exp\left(\frac{-E}{RT}\right)\right)dT+\frac{n}{2}\left(\int_{T_0}^{T}\left(\frac{A}{m}exp\left(\frac{-E}{RT}\right)\right)dT\right)^2+\cdots\right)\left(\Phi_{\text{P}}(E)+\Psi_{\text{p}}(E)\right)\\ +3\int_0^{\infty}&\left(1-\int_{T_0}^{T}\left(\frac{A}{m}exp\left(\frac{-E}{RT}\right)\right)dT+\frac{n}{2}\left(\int_{T_0}^{T}\left(\frac{A}{m}exp\left(\frac{-E}{RT}\right)\right)dT\right)^2+\cdots\right)\left(\Phi_{\text{P}}(E)+\Psi_{\text{p}}(E)\right)^2dE+\cdots.\end{aligned} \tag{22}$$

Applying Heaviside step function in Eq. (23), we have:

$$\begin{aligned}(1eX)_{n^{\text{th}}} \sim \int_0^{\infty}&\left(3E_0\left(1+\left[exp\left(\frac{y_{\text{s}}-y}{y_{\text{w}}}\right)-H(y-y_{\text{s}})\right]-\frac{n}{2}exp\left(2\left(\frac{y_{\text{s}}-y}{y_{\text{w}}}\right)-H(y-y_{\text{s}})\right)\right.\right.\\ &\left.+\cdots\right)\Big)d+3\int_0^{\infty}\left(1+\left[exp\left(\frac{y_{\text{s}}-y}{y_{\text{w}}}\right)-H(y-y_{\text{s}})\right]-\frac{n}{2}\left[exp\left(2\left(\frac{y_{\text{s}}-y}{y_{\text{w}}}\right)\right)-H(y-y_{\text{s}})\right]\\ &+\cdots\Bigg)\left(\left(\sqrt{\frac{\alpha}{\pi}}e^{-\alpha(y-1)^2}+\beta s^{\beta}(y)^{(\beta-1)}e^{-(sy)^{\beta}}\right)\right)\text{dy}+\int_0^{\infty}\left(1+\left[exp\left(\frac{y_{\text{s}}-y}{y_{\text{w}}}\right)-H(y-y_{\text{s}})\right]\right.\\ &-\frac{n}{2}\left[exp\left(2\left(\frac{y_{\text{s}}-y}{y_{\text{w}}}\right)\right)-H(y-y_{\text{s}})\right]+\cdots\Bigg)\frac{\alpha}{\pi}e^{-2\alpha(y-1)^2}dy+\int_0^{\infty}\left(1+\left[exp\left(\frac{y_{\text{s}}-y}{y_{\text{w}}}\right)\right.\right.\\ &\left.-H(y-y_{\text{s}})\right]-\frac{n}{2}\left[exp\left(2\left(\frac{y_{\text{s}}-y}{y_{\text{w}}}\right)\right)-H(y-y_{\text{s}})\right]+\cdots\Bigg)\beta s^{\beta}y^{(\beta-1)}e^{-2(sy)^{\beta}}dy\\ &+2\int_0^{\infty}\left(1+\left[exp\left(\frac{y_{\text{s}}-y}{y_{\text{w}}}\right)-H(y-y_{\text{s}})\right]-\frac{n}{2}\left[exp\left(2\left(\frac{y_{\text{s}}-y}{y_{\text{w}}}\right)-H(y-y_{\text{s}})\right.\right.\right.\\ &\left.\left.\left.+\cdots\right)\right]\left(\sqrt{\frac{\alpha}{\pi}}\right)\beta s^{\beta}(y)^{\beta-1}e^{-(\alpha(y-1)^2+(sy)^{\beta})}dy+\cdots\right).\end{aligned} \tag{23}$$

$$\sim\left(1-\frac{n}{2}\right)\Bigg[3\big((B_0+C_0)E_0-R(y_s)\big)+\frac{1}{2}\left(3+\sqrt{\frac{\alpha}{2\pi}}\right)erfc\left(\sqrt{\alpha}(y_s-1)\right)+(1-K)$$
$$+2(1-M)+3(1-S)+3\Bigg[\sqrt{\frac{\alpha}{\pi}}y_w e^{-\alpha(y_s-1)^2}\Big((B_0+C_0)-2\alpha y_w(y_s-1)(B_1+C_1)$$
$$+\alpha {y_w}^2\{2\alpha(y_s-1)^2-1\}(B_2+C_2)+\frac{2}{3}{y_w}^3\alpha^2\{2(y_s-1)+2\alpha(y_s-1)^3+1\}(B_3+C_3)\Big)$$
$$+\beta s^\beta\,(y_s)^{(\beta-1)}\exp\big(-(\alpha y_s)^\beta\big)\Big((B_0+C_0)-\frac{(y_w)}{y_s}\big(\beta-\beta(sy_s)^\beta-1\big)(B_1+C_1)$$
$$+\left(\frac{(y_w)}{y_s}\right)^2\big(\beta^2\big(-3(sy_s)^\beta+(sy_s)^{2\beta}+1\big)+3\lambda\big((sy_s)^\beta-1\big)+2\big)(B_2+C_2)$$
$$-\left(\frac{(y_w)}{y_s}\right)^3 A_3\left(s^2\beta^4(-{y_s}^2)\big((sy_s)^\beta-1\big)+\beta^3\big(-(sy_s)^2-7(sy_s)^\beta+3(sk_s)^{2\beta}+1\big)\right.$$
$$\left.-3\lambda^2\big(-6(sy_s)^\lambda+(sy_s)^{2\lambda}+2\big)-11\lambda\big((sy_s)^\lambda-1\big)-6\big)\right)\Bigg]+\left(1-\frac{n}{2}\right)\Bigg[\frac{\alpha}{\pi}y_w e^{-2\alpha(y_s-1)^2}\Big((B_0$$
$$+C_0)-4\alpha y_w(y_s-1)(B_1+C_1)+2\alpha {y_w}^2\{4\alpha(y_s-1)^2-1\}(B_2+C_2)+\frac{8}{3}{y_w}^3\alpha^2\{2(y_s-1)$$
$$+4\alpha(y_s-1)^3+1\}(B_3+C_3)\Big)+\Bigg(\beta^2 s^{2\beta}(y_s)^{2(\beta-1)}\exp\big(-(sy_s)^{2\beta}\big)\Big((B_0+C_0)$$
$$-2(B_1+C_1)\frac{y_w}{y_s}\big(\beta\big((sy_s)^\beta-1\big)+1\big)+(B_2+C_2)\left(\frac{y_w}{y_s}\right)^2\big(\beta^2\big(2+2(sy_s)^{2\beta}-5(sy_s)^\beta\big)$$
$$+5\beta\big((sy_s)^\beta-1\big)+3\big)+\frac{A_3}{3}\left(\frac{y_w}{y_s}\right)^3\big(\beta^3\big(4-4(sy_s)^{3\beta}+18(sy_s)^{2\beta}-19(sy_s)^\beta\big)$$
$$-9\beta^2\big(2+2(sy_s)^{2\beta}-5(sy_s)^\beta\big)-26\beta\big((sy_s)^\beta-1\big)-12\big)\Big)\Bigg]\Bigg]$$
$$+2\Bigg[\beta s^\beta\sqrt{\frac{\alpha}{\pi}}\Big((y_s)^{\beta-1}e^{-\left(\alpha(y_s-1)^2+(sy_s)^\beta\right)}\Big((B_0+C_0)+(B_1+C_1)\frac{y_w}{y_s}\big(-\beta(sy_s)^\beta+\beta$$
$$-2\alpha(y_s-1)y_s-1\big)+\frac{1}{2}(B_2+C_2)\left(\frac{y_w}{y_s}\right)^2\big(\beta^2\big(-3(sy_s)^\beta+(sy_s)^{2\beta}+1\big)+\beta(4\alpha y_s(y_s-1)$$
$$+3\big)\big((sy_s)^\beta-1\big)+4\alpha^2{y_s}^2(y_s-1)^2+2\alpha y_s(y_s-1)+2\big)+\frac{1}{6}(B_3$$
$$+C_3)\left(\frac{y_w}{y_s}\right)^3\Big)\Big(\beta^3\left(-\big(7(sy_s)^\beta-6(sy_s)^{2\beta}+(sy_s)^{3\beta}-1\big)\right)-6\beta^2(\alpha(y_s-1)y_s+1)\big(1$$
$$+(sy_s)^{3\beta}-3(sy_s)^\beta\big)-\beta(11+6y_s\alpha(2y_s-3)+12(y_s\alpha)^2(y_s-1)^2+6\alpha y_s(2y_s-3)$$
$$+11\big)\big((sy_s)^\beta-1\big)-2\left(4\big(\alpha y_s(y_s-1)\big)^3-6\big(\alpha y_s(y_s-1)\big)^2+3\alpha y_s(y_s-1)+3\right)\Big)+\cdots\Big)\Bigg]\Bigg].$$

3.4. Case D: n^{th} Order Reaction ($n \neq 1$) ($\theta = 2$)

$$(1-X)_{n^{\text{th}}}\sim\int_0^\infty\left[\left(1+\left(\frac{A}{m}exp\left(\frac{-E}{RT}\right)\right)+\frac{n}{2}\left(\frac{A}{m}exp\left(\frac{-E}{RT}\right)\right)^2+\cdots\right)dT\right]\Big(1-\big(\Phi_P(E)+\Psi_p(E)$$
$$+2\big)+\frac{3}{2}\big(\Phi_P(E)+\Psi_p(E)+2\big)^2+\cdots\Big),\qquad(25)$$

$$(16X)_{n^{\text{th}}}\sim\int_0^\infty\left[\left(1+exp\left(\frac{y_s-y}{y_w}\right)-\frac{n}{2}exp\left(2\left(\frac{y_s-y}{y_w}\right)\right)+\cdots\right)\right]\Big(5+5\left(\Phi_P(E)+\Psi_p(E)\right)$$
$$+\frac{3}{2}\left(\Phi_P(E)+\Psi_p(E)\right)^2+\cdots\Big).\qquad(26)$$

Using Heaviside step function in Eq. (27), we have:

$$
\begin{aligned}
(1(X)_{n^{\mathrm{th}}} \sim \left(1-\tfrac{n}{2}\right)\Big[\, & 5\big(A_0E_0+R(y_s)\big)+\tfrac{1}{2}\left(5+3\sqrt{\tfrac{\alpha}{2\pi}}\right)erfc\left(\sqrt{\alpha}(y_s-1)\right)+5(1-K)\\
&+\tfrac{3}{2}(1-M)\Big]+3(1-S)5\int_0^{\infty}\left(1+\left[exp\left(\tfrac{y_s-y}{y_w}\right)-H(y-y_s)\right]-\tfrac{n}{2}\left[exp\left(2\left(\tfrac{y_s-y}{y_w}\right)\right)\quad -H(y-y_s)\right]+\\
&\cdots\Big)dy+5\int_0^{\infty}\left(1+\left[exp\left(\tfrac{y_s-y}{y_w}\right)-H(y-y_s)\right]-\tfrac{n}{2}\left[exp\left(2\left(\tfrac{y_s-y}{y_w}\right)\right.\right.\right.\quad \left.\left.\left.-H(y-y_s)\right)\right]+\\
&\cdots\Big)\left(\sqrt{\tfrac{\alpha}{\pi}}e^{-\alpha(y-1)^2}+(sy)^{(\beta-1)}e^{-(sy)^{\beta}}\right)dy+\tfrac{3}{2}\left[\int_0^{\infty}\left(1+\left[exp\left(\tfrac{y_s-y}{y_w}\right)\right.\right.\right.\quad \left.\left.\left.-H(y-y_s)\right]-\right.\right.\\
&\left.\left.\tfrac{n}{2}\left[exp\left(2\left(\tfrac{y_s-y}{y_w}\right)-H(y-y_s)\right)\right]+\cdots\right)\tfrac{\alpha}{\pi}e^{-2\alpha(y-1)^2}dy+\int_0^{\infty}\left(1\quad +\left[exp\left(\tfrac{y_s-y}{y_w}\right)-H(y-y_s)\right]-\right.\right.\\
&\left.\left.\tfrac{n}{2}\left[exp\left(2\left(\tfrac{y_s-y}{y_w}\right)-H(y-y_s)\right)\right]\quad +\cdots\right)\tfrac{(\beta)^2s^{2\beta-1}y^{2\beta}}{\eta}e^{-2(sy)^{\beta}}dy\right]+3\int_0^{\infty}\left(1+\left[exp\left(\tfrac{y_s-y}{y_w}\right)-\right.\right.\\
&\left.\left.H(y-y_s)\right]-\tfrac{n}{2}\left[exp\left(2\left(\tfrac{y_s-y}{y_w}\right)\right.\right.\right.\quad \left.\left.\left.-H(y-y_s)+\cdots\right)\right]\left(\sqrt{\tfrac{\alpha}{\pi}}\right)\tfrac{\beta}{\eta}(sy)^{\beta-1}e^{-(\alpha(y-1)^2+(sy)^{\beta})}dy+\cdots\right).
\end{aligned}
\tag{27}
$$

$$
\begin{aligned}
\sim\left(1-\tfrac{n}{2}\right)\Bigg[& 5\big((B_0+C_0)E_0+R(y_s)\big)+\tfrac{1}{2}\left(5+3\sqrt{\tfrac{\alpha}{2\pi}}\right)erfc\left(\sqrt{\alpha}(y_s-1)\right)+5(1-K)\\
&+\tfrac{3}{2}(1-M)+3(1-S)+5\Bigg[\sqrt{\tfrac{\alpha}{\pi}}y_w e^{-\alpha(y_s-1)^2}\Big((B_0+C_0)-2\alpha y_w(y_s-1)(B_1+C_1)\\
&+\alpha {y_w}^2\{2\alpha(y_s-1)^2-1\}(B_2+C_2)+\tfrac{2}{3}{y_w}^3\alpha^2\{2(y_s-1)+2\alpha(y_s-1)^3+1\}(B_3+C_3)\Big)\\
&+\beta s^{\beta}\,(y_s)^{(\beta-1)}\exp\big(-(\alpha y_s)^{\beta}\big)\Big((B_0+C_0)-\tfrac{(y_w)}{y_s}\big(\beta-\beta(sy_s)^{\beta}-1\big)(B_1+C_1)\\
&+\left(\tfrac{(y_w)}{y_s}\right)^2\big(\beta^2\big(-3(sy_s)^{\beta}+(sy_s)^{2\beta}+1\big)+3\lambda\big((sy_s)^{\beta}-1\big)+2\big)(B_2+C_2)-\left(\tfrac{(y_w)}{y_s}\right)^3(B_3\\
&+C_3)\big(s^2\beta^4(-{y_s}^2)\big((sy_s)^{\beta}-1\big)+\beta^3\big(-(sy_s)^2-7(sy_s)^{\beta}+3(sk_s)^{2\beta}+1\big)-3\lambda^2\big(-6(sy_s)^{\lambda}\\
&+(sy_s)^{2\lambda}+2\big)-11\lambda\big((sy_s)^{\lambda}-1\big)-6\big)\Big)\Bigg]+\tfrac{3}{2}\Bigg[\tfrac{\alpha}{\pi}y_w e^{-2\alpha(y_s-1)^2}\Big((B_0+C_0)-4\alpha y_w(y_s\\
&-1)(B_1+C_1)+2\alpha {y_w}^2\{4\alpha(y_s-1)^2-1\}(B_2+C_2)+\tfrac{8}{3}{y_w}^3\alpha^2\{2(y_s-1)+4\alpha(y_s-1)^3\\
&+1\}(B_3+C_3)\Big)+\Bigg(\beta^2s^{2\beta}(y_s)^{2(\beta-1)}\exp\big(-(sy_s)^{2\beta}\big)\Big((B_0+C_0)-2(B_1+C_1)\tfrac{y_w}{y_s}\big(\beta\big((sy_s)^{\beta}\\
&-1\big)+1\big)+(B_2+C_2)\left(\tfrac{y_w}{y_s}\right)^2\big(\beta^2\big(2+2(sy_s)^{2\beta}-5(sy_s)^{\beta}\big)+5\beta\big((sy_s)^{\beta}-1\big)+3\big)\\
&+\tfrac{(B_3+C_3)}{3}\left(\tfrac{y_w}{y_s}\right)^3\big(\beta^3\big(4-4(sy_s)^{3\beta}+18(sy_s)^{2\beta}-19(sy_s)^{\beta}\big)-9\beta^2\big(2+2(sy_s)^{2\beta}-5(sy_s)^{\beta}\big)\\
&-26\beta\big((sy_s)^{\beta}-1\big)-12\big)\Big)\Bigg]+3\Bigg[\beta s^{\beta}\sqrt{\tfrac{\alpha}{\pi}}\Big((y_s)^{\beta-1}e^{-(\alpha(y_s-1)^2+(sy_s)^{\beta})}\Big((B_0+C_0)\\
&+(B_1+C_1)\tfrac{y_w}{y_s}\big(-\beta(sy_s)^{\beta}+\beta-2\alpha(y_s-1)y_s-1\big)+\tfrac{1}{2}(B_2+C_2)\left(\tfrac{y_w}{y_s}\right)^2\big(\beta^2\big(-3(sy_s)^{\beta}\\
&+(sy_s)^{2\beta}+1\big)+\beta\big(4\alpha y_s(y_s-1)+3\big)\big((sy_s)^{\beta}-1\big)+4\alpha^2{y_s}^2(y_s-1)^2+2\alpha y_s(y_s-1)+2\big)\\
&+\tfrac{1}{6}(B_3+C_3)\left(\tfrac{y_w}{y_s}\right)^3\Big)\Big(\beta^3\left(-\big(7(sy_s)^{\beta}-6(sy_s)^{2\beta}+(sy_s)^{3\beta}-1\big)\right)-6\beta^2(\alpha(y_s-1)y_s\\
&+1\big)\big(1+(sy_s)^{3\beta}-3(sy_s)^{\beta}\big)-\beta(11+6y_s\alpha(2y_s-3)+12(y_s\alpha)^2(y_s-1)^2\\
&+6\alpha y_s(2y_s-3)+11\big)\big((sy_s)^{\beta}-1\big)-2\left(4\big(\alpha y_s(y_s-1)\big)^3-6\big(\alpha y_s(y_s-1)\big)^2\right.\\
&\left.+3\alpha y_s(y_s-1)+3\big)\right)+\cdots\Big)\Bigg]\Bigg],
\end{aligned}
\tag{28}
$$

where the remaining integral terms are represented by:

$$A_i = \int_{-\infty}^{\infty} x^i \left(e^{-e^{-x}} - H(x)\right) dx,$$

$$B_i = \int_{-\infty}^{\infty} x^i \left(e^{-x} - H(x)\right)\ dx,$$

$$C_i = \int_{-\infty}^{\infty} x^i \left(e^{-2x} - H(x)\right)\ dx,$$

where $i = 0, 1, 2, 3, \ldots$.

These terms need to be evaluated once, as they are independent of any parameters and the first few values are:

$$A_0 \approx -0.5772, A_1 \approx -0.98906, A_2 \approx -1.81496,\ A_3 \approx -5.89037\ ,$$

$$B_0 \approx -0.36788, B_1 \approx -0.23576, B_2 \approx -0.17273, B_3 \approx -0.13607\ ,$$

$$C_0 \approx -0.56767,\ C_1 \approx -0.35150,\ C_2 \approx -0.25250,\ C_3 \approx -0.19642\ .$$

Here, α, *s*, *K*, *M*, *S* are defined as:

$$\alpha = \frac{{E_0}^2}{2\sigma^2} \text{ and } s = \frac{E_0}{\eta}\ ,$$

$$K = \int_{-\infty}^{y_s} e^{-2(sy)^\beta} \beta^2 s^{2\beta} y^{2(\beta-1)}\, dy,$$

$$M = \int_{-\infty}^{y_s} \beta s^\beta (y)^{\beta-1} e^{-\left(\alpha(y-1)^2 + (sy)^\beta\right)} dy,$$

$$S = \int_{-\infty}^{y_s} \beta s^\beta (y)^{\beta-1} e^{-(sy)^\beta} dy.$$

4. Application of Loose Biomass and the Computational Methodology

A pine needle sample is used to evaluate its thermal behavior and simulate the same results with the help of the mathematical model. To attain the pyrolysis conditions, nitrogen is used as a purge and protective gas to prevent the ingression of pollutants. Before initializing the experiment, the furnace space is purged to remove remaining oxygen. The volumetric rate of nitrogen 200 mL min^{-1} is employed to scavenge the product gases. Thermocouple type 'R' is used to measure the furnace temperature. The experiments were performed by using a thermogravimetric analyser (*SII* 6300 *EXSTAR*). The sample of 10.54 mg of pine needles is heated in a crucible pan of alumina at a heating rate of 10 °C min^{-1}. To prevent the buoyancy effect, correction measurements are used. Elemental analysis of the pine needles is carried out with the help of CHNO-S analyser (*FLASH EA* 1112 series). Table 1 illustrated the elemental composition of pine needles on the dry basis. Calorific value is derived through bomb calorimeter at constant volume.

On the other hand, it is to be noted that thermoanalytical data is used to evaluate the predicted results from the multivariate n^{th} order DAEM. To simulate the results, the mean square error between the mathematical and experimental values is minimized with the help of the designed algorithm on the *MATLAB* software. The objective functions for each case of this computational problem are Eq. (17), Eq. (21), Eq. (25) and Eq. (29). Each assigned value is derived after comparing the mean square error with maximum permissible error while running every iterative loop. Unless the estimated value agrees with the end conditions, the iterative loop searches for another value. At the end of the program, the kinetic parameters are evaluated.

TABLE 1. CHEMICAL COMPOSITION OF PINE NEEDLES (DRY BASIS)

C, %	H, %	N, %	O, %	S, %	Ash, %	H.H.V.*, MJ/kg	V. M.**, %
53.7	5.21	0.61	32.13	0.22	4.72	19.5	70.1

*Higher heating value; **Volatile matter.

5. RESULTS AND DISCUSSION

The Clayton copula is applied to solve the multi reaction model (MRM) or distributed activation energy model (DAEM). Here, the initial distribution function is replaced by the bivariate function $f(E_1, E_2)$ that is a combination of the asymmetric (Weibull) and symmetric (Gaussian) so that the attribute of both functions can be exploited in our objective functions. Copula parameters (θ), scale (η) and shape parameters (β), reaction order (n), frequency factor (A), heating rate (m) and the upper limit (E_∞) of 'dE' integral are some of the relevant parameters considered to reproduce good pyrolysis behavior. The numerical solutions for different classes of copula parameters (θ) are derived with the help of the step-function $H(y–y_s)$. Furthermore, each class is bifurcated into the first and n^{th} order reactions.

In the initial stage of biomass pyrolysis, the remaining mass fraction must be in the vicinity of one, whereas it has been seen that the remaining mass proportion is more than one for all the values of upper limits beyond $661.7 \geq E_\infty$ (kJ/mol) as illustrated in Fig. 1(a, b). On the other hand, there is no solution obtained for the higher value of copula parameter $\theta \geq 2$ (Fig. 1(c, d)). Moreover, the conversion of biomass with respect to temperature increases with the decrease in the upper limit beyond $E_\infty \leq 146.28$ kJ/mol. It implies conversion of biomass occurs instantaneously without appreciable temperature gradients, but in a practical aspect due to limitations of heat transfer between specimen and furnace which take some time to establish equilibrium with temperature of the sample [37]. Therefore, this domain of upper limit $E_\infty \leq 146.28$ kJ/mol cannot be a solution of the given problem. Influence of the higher value of the copula parameter made the objective function strictly increase for all the values of $E \in N$, hence, there is no solution in the domain of the upper limit $649.87 \text{ kJ/mol} \leq E_\infty < \infty$. Another reason for the anomaly in the behavior of $(1–X)$ is the limit applied to the Clayton copula. In the beginning, the whole integrand follows the trail of Clayton copula, but as time proceeds, $(1–X)$ curves converge with an increase in the temperature scale. Moreover, it is also observed that the decrease in the upper limit of E_∞ caused $(1–X)$ curves to lead toward the left-hand side. For $\theta \geq 2$, the 398 kJ/mol can be used as the upper limit E_∞ of activation energy. In case of the independent copula ($\theta \geq 1$), the upper limit is found to be 655 kJ/mol.

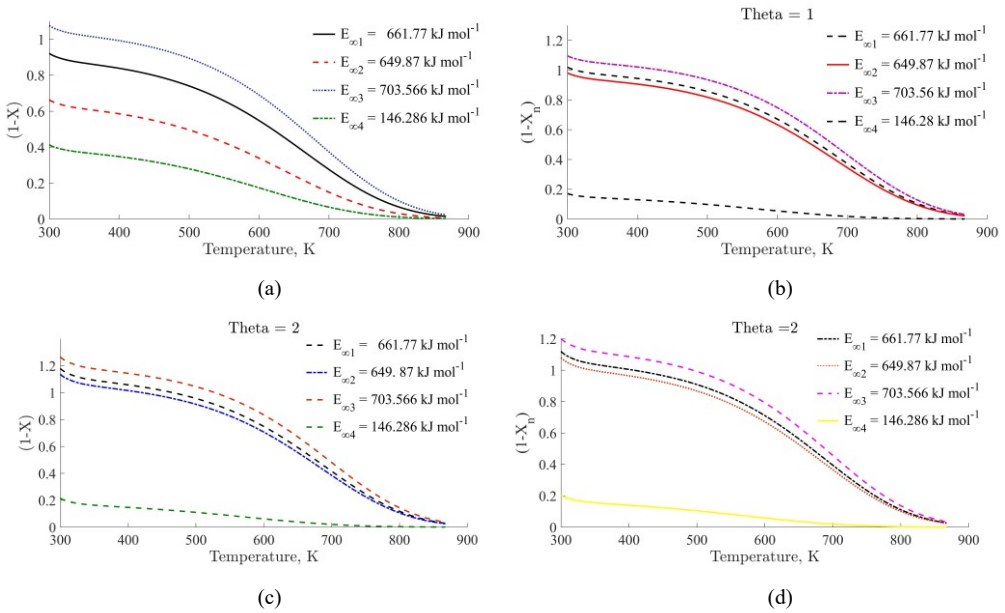

Fig. 1. The effect of upper limit $'E_{\infty}'$ (kJ mol^{-1}) of dE integral on the numerical solutions of bi-variant scheme for distributed activation energy model (DAEM): (a) first order reaction ($\theta = 1$); (b) n^{th} order reaction ($\theta = 1$); (c) first order reaction ($\theta = 2$); (d) n^{th} order reaction ($\theta = 2$) ($A = 1.5 \cdot 10^{-005}$ s^{-1}, $\eta = 10^{-9}$ kJ/mol, $\beta = 0.0920$, $m = 10$ °C min^{-1} and $n = 0.11$).

The effect of frequency factor A on the numerical results at different values of θ is depicted in Fig. 2(a, c, d). The remaining mass proportion curves ($1–X$) resulted in a downward shift with decrease in the frequency factor, however, the variation in numerical solutions obtained at the small interval of A is negligibly small. As the value of frequency factor increases, the remaining mass fraction curve becomes greater than one. Therefore, in case of the Clayton copula, the frequency factor not only affects the characteristic of curves but also changes the end conditions. It is computed that the domain of frequency factor must lie in the interval $10^{-5} < A$ (s^{-1}) $\leq 1.5 \cdot 10^{-5}$. The curve fitting is derived for all the values of scale parameter (η) which was found to lie in the domain of 10^{-11} kJ/mol $\leq \eta < 10^{-08}$ kJ/mol for independent copula in Fig. 3(a, b). On the other hand, the upper limit of interval shrinks for the higher values of copula parameters 10^{-11} kJ/mol $\leq \eta < 10^{-09}$ kJ/mol as shown in Fig. 3(c, d). Similarly, the effect of scale parameter is not merely confined to change in attribute of remaining mass fraction but also influences its upper limit. The effect of shape parameter on the numerical solution is illustrated in Fig. 4(a–d). The remaining mass fraction is more than one for all the values $0.0520 \geq \beta$. Hence, the domain of shape parameter for the given non-isothermal problems lies in the interval of $0.0720 \leq \beta \leq 0.090$. The effect of heating rate (m) on the numerical solution is illustrated in Fig. 5(a–d). In case of heating rate, the variation among different heating rate is infinitesimally small, and therefore, all the curves completely overlap with each other. Mathematical perturbation, in case of Clayton copula, exhibited non-perceivable observation. Influence of reaction order (n) due to variation of copula parameters is depicted in Fig. 6(a–d). The values of ($1–X$) curves show proximity with each other for all the values of n lying in an interval of $0.1 \leq n \leq 1$.

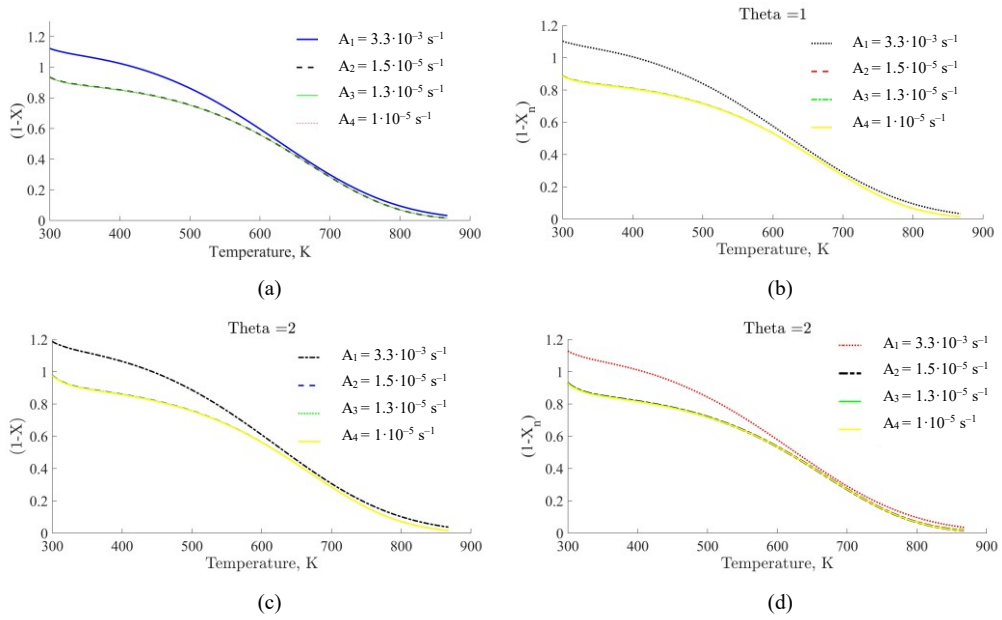

Fig. 2. The effect of frequency factor (A) (s^{-1}) on the numerical results of bi-variant scheme for DAEM: (a) first order reaction ($\theta = 1$); (b) n^{th} order reaction ($\theta = 1$); (c) first order reaction ($\theta = 2$); (d) n^{th} order reaction ($\theta = 2$) ($\eta = 10^{-9}$ kJ/mol, $\beta = 0.0920$, $m = 10$ °C min^{-1} and $n = 0.11$).

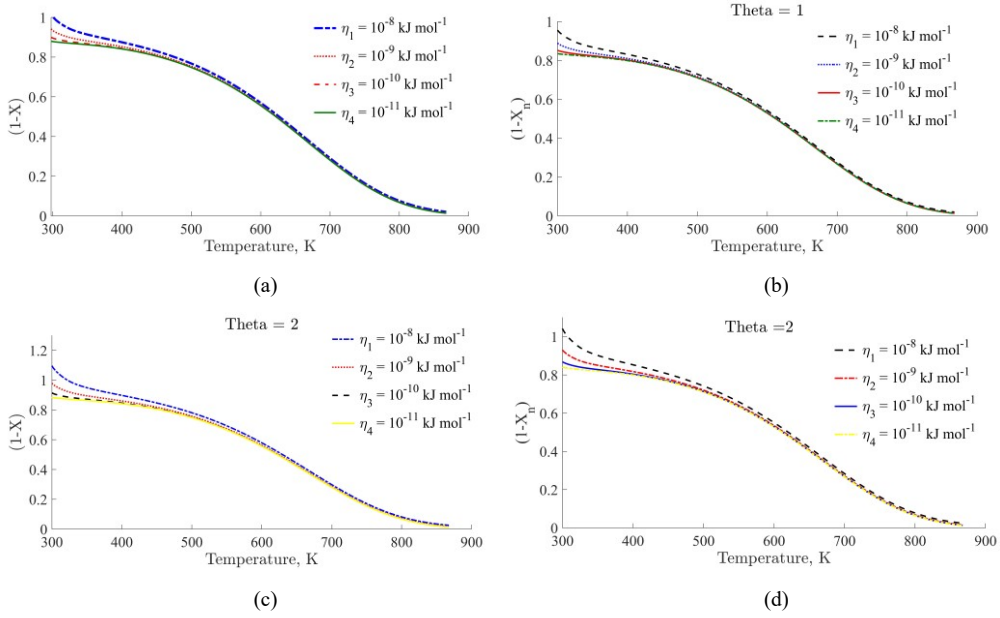

Fig. 3. The effect of scale parameter (η (kJ mol^{-1})) of the Weibull distribution on the numerical results of bi-variant scheme for DAEM: (a) first order reaction ($\theta = 1$); (b) n^{th} order reaction ($\theta = 1$); (c) first order reaction ($\theta = 2$); (d) n^{th} order reaction ($\theta = 2$) ($A = 1.5 \cdot 10^{-005}\ s^{-1}$, $\beta = 0.0920$, $m = 10$ °C min^{-1} and $n = 0.11$).

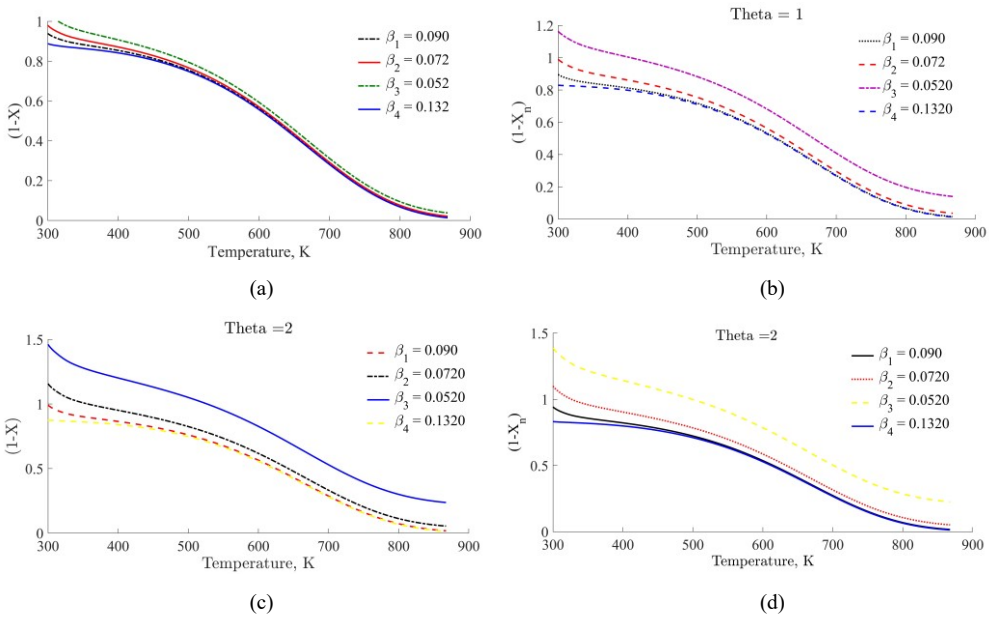

Fig. 4. The effect of shape parameter (β) of the Weibull distribution on the numerical results of bi-variant scheme for DAEM: (a) first order reaction ($\theta = 1$); (b) n^{th} order reaction ($\theta = 1$); (c) first order reaction ($\theta = 2$); (d) n^{th} order reaction ($\theta = 2$) ($A = 1.5 \cdot 10^{-005}\ s^{-1}$, $\eta = 10^{-9}$ kJ/mol, $m = 10$ °C min^{-1} and $n = 0.11$).

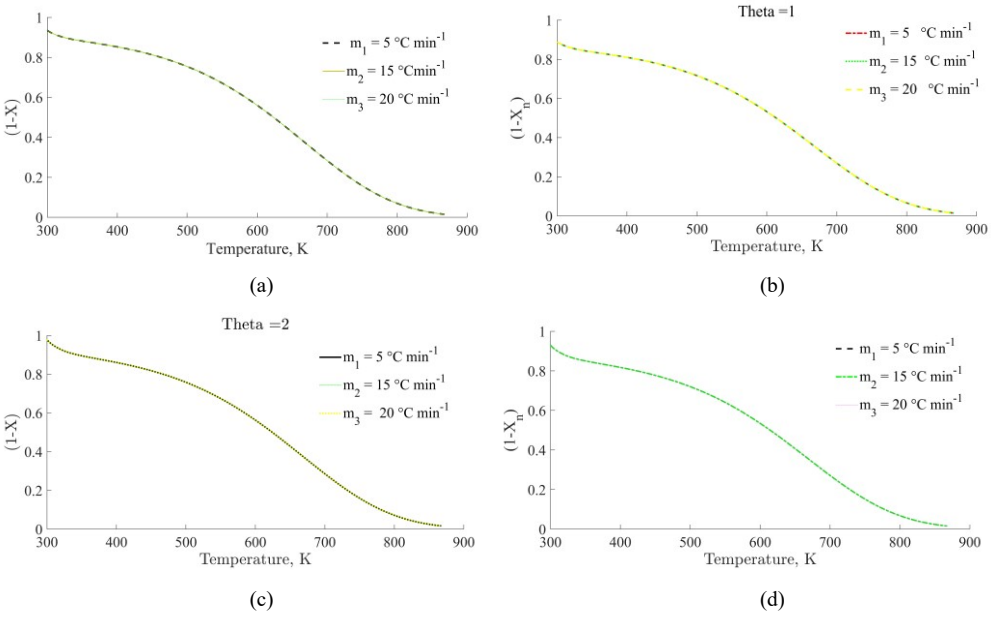

Fig. 5. The effect of heating rate (m (°C min^{-1})) on the numerical results of bi-variant scheme for DAEM: (a) first order reaction ($\theta = 1$); (b) n^{th} order reaction ($\theta = 1$); (c) first order reaction ($\theta = 2$); (d) n^{th} order reaction ($\theta = 2$) ($A = 1.5 \cdot 10^{-005}\ s^{-1}$, $\eta = 10^{-9}$ kJ/mol, $\beta = 0.0920$, and $n = 0.11$).

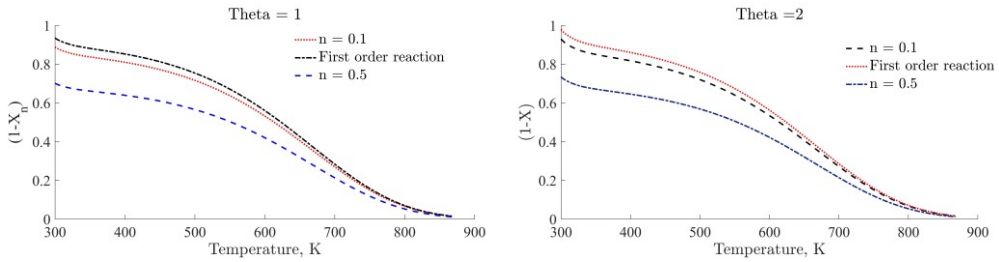

(a) (b)

Fig. 6. The effect of reaction order (n) on the numerical results of bi-variant scheme for DAEM: (a) $\theta = 1$; (b) $\theta = 2$ ($A = 1.5 \cdot 10^{-005}$ s^{-1}, $\eta = 10^{-9}$ kJ/mol, $m = 10$ °C min^{-1} and $\beta = 0.0920$).

Comparison of thermoanalytical data with predicted n^{th} order DAEM is demonstrated in Fig. 7. It can be observed that the Clayton copula has properly grasped the two separate steps of pyrolysis as compared to the univariant scheme for the same material (Fig. 8). There is relatively great improvement in the curve fitting at the onset of the pyrolysis process. It is clear from the TG curves of pine needles that the first half of the curve refers to the primary stage which is extended from 500 K to 650 K; whereas the second regimes represents the higher ones (600–900 K). The 80 % of volatile component is released during the primary stage which perfectly coincides in case of the bivariate scheme. On the other hand, the univariate scheme (Fig. 8(a, b)) is not able to predict more precisely the primary region than the n^{th} order prediction DAEM using the Clayton copula, however, there are some demerits related to the bivariate scheme, as it is not able to assess the behavior of the remaining mass proportion with respect to heating rate. In case of different types of univariate functions, the parameters are merely influenced by the attribute of curves rather than intervening in the domain of some relevant parameters [20]–[25]. Due to the introduction of two different natures of distribution functions, the effect of inflexion points as well as effect of DExp on the final solution is reduced and the whole pattern is shifted to the right, which, in turn, helped to exhibit slow pyrolysis through mathematical modelling. It can be concluded that the Clayton copula has provided a good insight into a model two-step process of pyrolysis, as well as a combined effect of two different patterns.

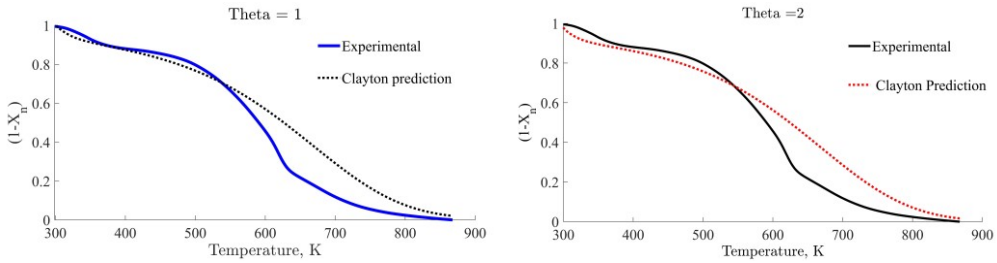

(a) (b)

Fig. 7. Comparison between experimental data and the n^{th} order bi-variant scheme for DAEM: (a) $\theta = 1$; (b) $\theta = 2$.

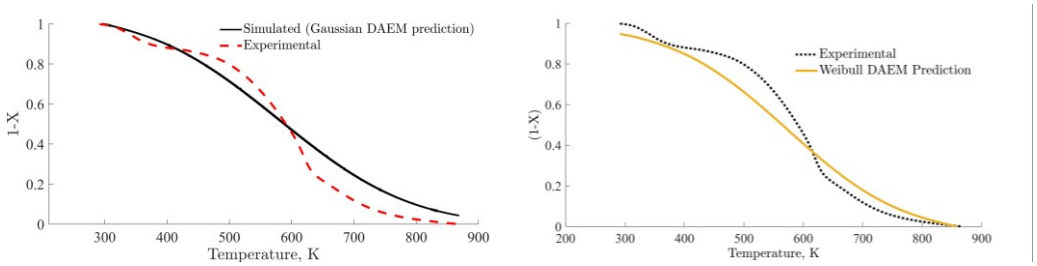

(a) (b)

Fig. 8. Comparison between experimental data and the n^{th} order DAEM prediction (Univariate scheme): (a) Gaussian; (b) Weibull.

6. CONCLUSIONS

In this paper, a bivariate scheme has been adopted to overcome the inadequacy of the univariate model to properly describe both pyrolysis steps. This proposed method is used to predict the best possible outcome for the given thermoanalytical data. The Clayton copula, as a bivariate function, is also compared to a univariate method so that it overcomes the shortcoming of univariate functions. The results of fitting show that E_∞ = 655 kJ/mol can be used as the upper limit for θ = 1; whereas the upper limit of E_∞=398 kJ/mol is for θ = 2. Similarly, the frequency factor $A(s^{-1})$ = 1.5E–05 is found to be a common solution for all the values of $1 \leq \theta \leq 2$. The values of distribution parameters, scale and shape parameters are estimated to be $\eta = 10^{-10}$ kJ/mol and β = 0.081, respectively. The range of reaction order for the Clayton copula is estimated to be $0.1 \leq n \leq 1$. The result produced by the Clayton copula has shown that the primary pyrolysis is the predominant phase in biomass pyrolysis, taking place at the higher activation range. Besides the evaluation of kinetic parameters and prediction, the two important facts that came into light are that the Clayton copula does not perceive variation in the final solution with respect to the heating rate (m) and distribution parameters, and that the frequency factor not only influences the attribute but also the end conditions of the remaining mass fraction curves.

ACKNOWLEDGEMENT

This work was supported by the Stipendium Hungaricum Programme and by the Mechanical Engineering Doctoral School, Szent István University, Gödöllő, Hungary.

APPENDIX A

For our application $0 < \theta < \infty$, so this can be simplified as:

$$C_\theta\left(f(E_1);\, f(E_2)\right) = \left(\left(\Phi_{\mathrm{P}}(\mathrm{E})\right)^{-\theta} + \left(\Psi_{\mathrm{p}}(\mathrm{E})\right)^{-\theta} - 1\right)^{-\left(\frac{1}{\theta}\right)},$$

$$C_\theta\left(f(E_1);\, f(E_2)\right) = \left(\left(1 - (\Phi_{\mathrm{P}}(\mathrm{E}) + 1)\right)^{-\theta} + \left(1 - \left(\Psi_{\mathrm{p}}(\mathrm{E}) + 1\right)\right)^{-\theta} - 1\right)^{-\left(\frac{1}{\theta}\right)}. \quad \text{(A1)}$$

Apply binomial theorem to the first and the second terms of Eq. (A1), we have:

$$\sim\left(\left(1+\theta(\Phi_{\mathrm{P}}(\mathrm{E})+1)+\frac{\theta(\theta+1)}{2}(\Phi_{\mathrm{P}}(E)+1)^2+..\right)+\theta\left(\Psi_{\mathrm{p}}(\mathrm{E})+1\right)+\frac{\theta(\theta+1)}{2}\left(\Psi_{\mathrm{p}}(E)+1\right)^2\right)^{-\left(\frac{1}{\theta}\right)}. \quad \text{(A2)}$$

After simplification of Eq. (A2), we have:

$$\sim\left(1+\theta\left(\Phi_{\mathrm{P}}(\mathrm{E})+\Psi_{\mathrm{p}}(\mathrm{E})+2\right)\right)^{-\left(\frac{1}{\theta}\right)}. \quad \text{(A3)}$$

Expand the Eq. (A3) with the help of binomial theorem, we get:

$$\sim\left(1-\left(\Phi_{\mathrm{P}}(E)+\Psi_{\mathrm{p}}(E)+2\right)+\frac{(\theta+1)}{2}\left(\Phi_{\mathrm{P}}(E)+\Psi_{\mathrm{p}}(E)+2\right)^2+\cdots\right). \quad \text{(A4)}$$

Solve the generalised form of Eq. (A4), we get two different cases for the different values of Copula parameter (θ).

Case I: $\theta = 1$:

$$\sim\left(1-\left(\Phi_{\mathrm{P}}(E)+\Psi_{\mathrm{p}}(E)+2\right)+\left(\Phi_{\mathrm{P}}(E)+\Psi_{\mathrm{p}}(E)+2\right)^2+\cdots\right). \quad \text{(A5)}$$

Case II: $\theta = 2$:

$$\sim\left(1-\left(\Phi_{\mathrm{P}}(\mathrm{E})+\Psi_{\mathrm{p}}(\mathrm{E})+2\right)+\frac{3}{2}\left(\Phi_{\mathrm{P}}(\mathrm{E})+\Psi_{\mathrm{p}}(\mathrm{E})+2\right)^2\right). \quad \text{(A6)}$$

Eq. (A5) and Eq. (A6) are the required approximated expression for Clayton copula.

REFERENCES

[1] Dhaundiyal A., Gupta V. K. The Analysis of Pine Needles as a Substrate for Gasification. *J. Water Energy Environ*. 2014:15:73–81. doi:10.3126/hn.v15i0.11299

[2] Dhaundiyal A., Tewari P. C. Comparative analysis of pine needles and coal for electricity generation using carbon taxation and emission reductions. *Acta Technol. Agric*. 2015:18(2):29–35. doi:10.1515/ata-2015-0007

[3] Dhaundiyal A., Tewari P. C. Performance evaluation of throatless gasifier using pine needles as a feedstock for power generation. *Acta Technol. Agric*. 2016:19(1):10–18. doi:10.1515/ata-2016-0003

[4] Dhaundiyal A., Singh S. B. Distributed activation energy modelling for pyrolysis of forest waste using gaussian distribution. *Proc. Latv. Acad. Sci. Sect. B* 2016:70(2):64–70. doi:10.1515/prolas-2016-0011

[5] Dhaundiyal A., Tewari P. C. Kinetic Parameters for the Thermal Decomposition of Forest Waste Using Distributed Activation Energy Model (DAEM). *Environment and Climate Technologies* 2017:19(1):15–32. doi:10.1515/rtuect-2017-0002

[6] Kader M. A., Islam M. R., Parveen M., Haniu H., Takai K. Pyrolysis decomposition of tamarind seed for alternative fuel. *Bioresour. Technol*. 2014:149:1–7. doi:10.1016/j.biortech.2013.09.032

[7] Gaqa S., Mamphweli S., Katwire D., Meyer E. Synergistic evaluation of the biomass/coal blends for cogasification purposes. *Int. J. Energy Environ. (IJEE)* 2014:5(2):251–256.

[8] Vyazovkin S., Wight C. A. Model-free and model-fitting approaches to kinetic analysis of isothermal and nonisothermal data. *Thermochimica acta* 1999:340–341:53–68. doi:10.1016/S0040-6031(99)00253-1

[9] Capart R., Khezami L., Burnham A. K. Assessment of various kinetic models for the pyrolysis of a microgranular cellulose. *Thermochim. Acta* 2004:417(1):79–89. doi:10.1016/j.tca.2004.01.029

[10] Conesa J. A., Caballero J. A., Marcilla A., Font R. Analysis of different kinetic models in the dynamic pyrolysis of cellulose. *Thermochim. Acta* 1995:254:175–192. doi:10.1016/0040-6031(94)02102-T
[11] Conesa J. A., Marcilla A., Caballero J. A., Font R. Comments on the validity and utility of the different methods for kinetic analysis of thermogravimetric data. *J. Anal. Appl. Pyrolysis* 2001:58–59:617–633. doi:10.1016/S0165-2370(00)00130-3
[12] Pysiak J. J., Al.-Badwi Y. A. Kinetic equations for thermal dissociation processes. *J. Therm. Anal. Calorim*. 2004:76(2):521–528. doi:10.1023/B:JTAN.0000028030.49773.ad
[13] Yaroshenko A. P. Theoretical model and experimental study of pore growth during thermal expansion of graphite intercalation compounds. *J. Therm. Anal. Calorim*. 2005:79(3):515–519. doi:10.1007/s10973-005-0571-3
[14] Criado J. M., Perez-Maqueda L. A. Sample controlled thermal analysis and kinetics. *J. Therm. Anal. Calorim*. 2005:80(1):27–33. doi:10.1007/s10973-005-0609-6
[15] Burnham A. K., Braun R. L. Global kinetic analysis of complex materials. *Energy Fuels* 1999:13(1):1–22. doi:10.1021/ef9800765
[16] Burnham A. K., Schmidt B. J., Braun R. L. A test of parallel reaction model using kinetic measurements on hydrous pyrolysis residues. *Org. Geochem.* 1995:23(10):931–939. doi:10.1016/0146-6380(95)00069-0
[17] Galgano A., Blasi C. D. Modeling Wood Degradation by the Unreacted-Core-Shrinking Approximation. *Ind. Eng. Chem. Res*. 2003:42(10):2101–2111. doi:10.1021/ie020939o
[18] Ferdous D., Dalai A. K., Bej S. K., Thring R. W. Pyrolysis of Lignins: Experimental and Kinetics Studies. *Energy Fuels* 2002:16(6):1405–1412. doi:10.1021/ef0200323
[19] Dhaundiyal A., Singh S. B. Mathematical insight to non-isothermal pyrolysis of pine needles for different probability distribution functions. *Biofuels* 2017:1–12. doi:10.1080/17597269.2017.1329495
[20] Cai J. M., He F., Yao F. S. Non-isothermal nth-order DAEM equation and its parametric study – Use in the kinetic analysis of biomass pyrolysis. *J. Math. Chem*. 2006:42(4):949–956. doi:10.1007/s10910-006-9151-4
[21] Dhaundiyal A., Singh S. B. Asymptotic approximations to the distributed activation energy model for non-isothermal pyrolysis of loose biomass using the weibull distribution. *Arch. Combust*. 2016:36(2):131–146.
[22] Dhaundiyal A., Singh S. B. Approximations to the Non-Isothermal Distributed Activation Energy Model for Biomass Pyrolysis Using the Rayleigh Distribution. *Acta Technol. Agric*. 2017:20(3):78–84. doi:10.1515/ata-2017-0016
[23] Dhaundiyal A., Singh S. B. Implementation of Fuzzy Sets in the Non-Isothermal Pyrolysis of Biomass. *J. Nat. Resour. Dev*. 2017:7:30–37.
[24] Niksa S., Lau C. W. Global rates of devolatilization for various coal types. *Combus. Flame* 1993:94(3):293–307. doi:10.1016/0010-2180(93)90075-E
[25] Dhaundiyal A., Singh S. B. Parametric Study of n^{th} Order Distributed Activation Energy Model for Isothermal Pyrolysis of Forest Waste Using Gaussian Distribution. *Acta Technologica Agriculturae* 2017:20(1):23–28. doi:10.1515/ata-2017-0005
[26] Howard J. B. Fundamentals of Coal Pyrolysis and Hydropyrolysis: Chemistry of Coal Utilization. New York: John Wiley and Sons, 1981.
[27] Vand V. Theory of the irreversible electrical resistance changes of metallic films evaporated in vacuum. *Proc. Phys. Soc. Lond. A* 1943:55(3):222–246.
[28] Pitt G. J. The kinetics of the evolution of volatile products from coal. *Fuel* 1962:41:267–274.
[29] Suuberg E. M. Approximate solution technique for nonisothermal, Gaussian distributed activation energy models. *Combust. Flame* 1983:50:243–245. doi:10.1016/0010-2180(83)90066-4
[30] Kumar D., Singh S. B. Stochastic Analysis of Complex Repairable System with Deliberate Failure Emphasizing Reboot Delay. *Commun. Stat. Simul. Comput*. 2016:45(2):583–602. doi:10.1080/03610918.2013.867993
[31] Mangey R., Singh S. B., Singh V. V. Stochastic Analysis of a Standby System with waiting repair strategy. *IEEE Trans. Syst. Man Cybern. Syst.* 2013:43(3):698–707. doi:10.1109/TSMCA.2012.2217320
[32] Nailwal B., Singh S. B. Performance evaluation and reliability analysis of a complex system with three possibilities in repair with the application of copula. *Int. J. Reliab. Appl*. 2011:12(1):15–39.
[33] Oakes D. On the preservation of copula structure under truncation. *Can. J. Stat*. 2005:33(3):465–468. doi:10.1002/cjs.5540330310
[34] de Caprariis B., de Filippis P., Herce C., Verdone N. Double-gaussian distributed activation energy model for coal devolatilization. *Energy Fuels* 2012:26(10):6153–6159. doi:10.1021/ef301092r
[35] Zhang J., Chen T., Wu J., Wu J. Multi-Gaussian-DAEM-reaction model for thermal decompositions of cellulose, hemicellulose and lignin: Comparison of N_2 and CO_2 atmosphere. *Bioresour. Technol*. 2014:166:87–95. doi:10.1016/j.biortech.2014.05.030
[36] Yang X., Zhang R., Fu J., Geng S., Cheng J. J., Sun Y. Pyrolysis kinetic and product analysis of different microalgal biomass by distributed activation energy model and pyrolysis–gas chromatography–mass spectrometry. *Bioresour. Technol*. 2014:163:335–342. doi:10.1016/j.biortech.2014.04.040
[37] Quan C., Li A., Gao N. Thermogravimetric analysis and kinetic study on large particles of printed circuit board wastes. *Waste Management* 2009:29(8):2353–2360. doi:10.1016/j.wasman.2009.03.020

Alok Dhaundiyal. In 2014, he had been awarded the master's degree in mechanical engineering from GBPUAT, Uttarakhand, India. From 2015 to 2017, he worked as an Assistant Professor in Himgiri Zee University. He has also worked on Deutsche Gesellschaft für Internationale Zusammenarbeit (GIZ) projects, which are the part of Indo-German Govt. Programme to promote renewable energy sector of India under the patronage of state government agency of Uttrakhand, India, UREDA; and Central ministry, Ministry of New Renewable Energy. Author's area of expertise is the energy generation through the biomass waste utilization. In 2012, he has been awarded the Graduate Aptitude Test Engineering (GATE) Scholarship for Master of Engineering by the govt. of India. The Faculty of Engineering Excellence award has been conferred on him by the University of Strathclyde, Scotland, United Kingdom. He has also received the University Grant Commission (2017 to 2022) scholarship. In 2017, the Stipendium Hungaricum Scholarship has been bestowed upon him by the government of Hungary. Currently, he is the doctoral student (Mechanical) in Szent István Egyetem (St. Stephen University), Hungary. ORCID: 0000-0002-3390-0860.

Dr. S. B. Singh is a Professor in the Department of Mathematics, Statistics and Computer Science, G. B. Pant University of Agriculture and Technology, Pantnagar (Uttarakhand), India. He has around 24 years of teaching and research experience to Undergraduate and Post Graduate students at different Engineering Colleges and University. Prof. Singh is a member of Indian Mathematical Society, Operations Research Society of India, Member of Advisory board of Intellectual Society for Socio-Techno Welfare (ISST) and National Society for Prevention of Blindness in India and Member of Indian Science Congress Association. He is a regular reviewer of many books and International/ National Journals. Prof. Singh has been a member of organizing committee of many international and national conferences and workshops. He is an Editor of the 'Journal of Reliability and Statistical Studies'. He is member of Editorial board of seven journals and edited books as well. He has authored and coauthored eight books on different courses of Applied/ Engineering Mathematics. Prof. Singh has been conferred with five national awards and the Best Teacher Award. He has been included in the special edition of Marquis Who's Who in the World 2015, USA. Prof. Singh has been member of Research Advisory Committee of many M.Sc. (Maths, Physics and Chemistry), Ph. D. (Maths, Physics, Engineering, Management, Home Science) and M.Tech students. His area of research is Reliability Theory/Engineering.

Muammel M. Hanon is currently PhD student in Mechanical Engineering at Szent Istvan University (Hungary) and obtained the master's degree in the field of Laser/Mechanical Engineering from University of Baghdad (Iraq) in 2011. He completed the B.Sc. degree in Mechanical Engineering at the university of Technology/Baghdad in 2007. He works as a lecturer since 2011 at the Middle Technical University, Iraq. He has also worked as the manager of IDs issuing department in Iraqi Engineers Union for 7 years (2007–2014). He has some publications in International journals e.g. (Experimental and theoretical investigation of the drilling of alumina ceramic using Nd:YAG pulsed laser, J. Opt. Laser Technol., doi:10.1016/j.optlastec.2011.11.010.) and (Laser welding of copper with stellite 6 powder and investigation using LIBS technique, J. Opt. Laser Technol., doi:10.1016/j.optlastec.2012.05.001). The Author is a member of "Arab Engineers Union" and "Iraqi Engineers Union". In 2017, He received the Stipendium Hungaricum award granted by the government of Hungary. Author's research area entails laser materials processing, renewable energy, and tribology of 3D printed polymers.
ORCID: 0000-0003-4811-5723.

Norbert Attila Schrempf PhD graduated from Agricultural Mechanical Engineering in 2000, received a VET degree from Logistics and Quality Management in 2001. He received his PhD degree from Agricultural Mechanical Science at Godollo in 2007.
Work experiences: Visiting Scientist at the MTA, Instructor, Manager of Agricultural Energetics, Mechanical Management and Energetic Specializations, Energy Management VET, Head of Energetics Specialization, Vice Director of the Institute of Process Engineering at Szent István University Godollo.
Last publication: Toth L, Madar V, Bacskai I, Schrempf N (2017): Biomassza-pirolízis alapú kiserőmű fejlesztése. His researches are mainly about energetics and renewable energy sources.
He is a member of: Hungarian Wind Energy Scientific Society, Agricultural Mechanical Committee of the MTA, Hungarian Wind Energy Society; European Wind Energy Association, World Wind Energy Association.